Journal of Hazardous Materials 162 (2009) 237–248

Contents lists available at ScienceDirect

Journal of Hazardous Materials

journal homepage: www.elsevier.com/locate/jhazmat

Analyzing a liquid–solid phase countercurrent two- and three-stage adsorption process with the Freundlich equation

Ru-Ling Tseng [a], Feng-Chin Wu [b,*]

[a] Department of Safety, Health and Environmental Engineering, National United University, Miao-Li 360, Taiwan
[b] Department of Chemical Engineering, National United University, No. 1, Lien Da, Kung-Ching Li, Miao-Li 360, Taiwan

ARTICLE INFO

Article history:
Received 28 January 2008
Received in revised form 6 May 2008
Accepted 6 May 2008
Available online 14 May 2008

Keywords:
Activated carbon
Countercurrent multi-stage
Adsorption process
Freundlich equation
Process design

ABSTRACT

Adsorbent consumption advantages of a countercurrent two- and three-stage process are described. The Freundlich equation and equilibrium-stage were used to deduce these adsorption processes; it was proved that large adsorbent savings were obtained from operations of these systems in most cases. Microporous activated carbon was prepared from plum kernels with KOH chemical activation. Isotherm equilibrium adsorptions of three dyes (BB1, MB, and AB74) and three phenols (phenol, 4-CP, and 2,4-DCP) were used to explain both the superior adsorption capability of activated carbon and the advantages of analyzing adsorption system operations with the Freundlich equation, and to calculate the countercurrent two- and three-stage adsorption processes and explain the design procedures. A continuous-flow countercurrent three-stage adsorption process was developed to provide for design in practical application.

1. Introduction

Adsorption with activated carbon is widely employed for the removal of organic matter in water purification. Several adsorber configurations are possible for activated carbon treatment; these include the batch vessel, the continuous-flow stirred tank, the fixed bed, the moving bed, and the fluidized bed. Traditionally, the treatment of choice has been packed-bed adsorption because of the ease and reliability of this operation. Nevertheless, several problems, such as excessive head loss, air binding, and fouling with biological and particulate matter are associated with packed-bed operation [1].

In theory, the adsorption capability of an adsorbent can be fully developed with packed-bed adsorption and an ideal countercurrent adsorption process. But because of the difficulties mentioned above, packed-bed adsorption is not suitable for practical applications; furthermore, it is also difficult to design a complete liquid–solid phase countercurrent adsorption process. Thus, some designs for a simulated moving-bed adsorber have been suggested. The multiple-pipe moving-bed adsorber is, in function, close to the countercurrent adsorption process [2–8], and thus can be used in the purification of biotech products (e.g. glucose-salts, glucose/fructose) [9–16]. Simulated moving-bed adsorbers, expensive and complicated structures, are used in making high price products; however, they are not usually used in adsorption systems of low operation cost, such as wastewater treatment.

Many agricultural wastes can be converted into adsorbent, which cannot be used in packed-bed because of their poor operation; thus, batch stirred tanks are necessary for adsorption. Countercurrent two- and three-adsorption processes were used in this study, together with the Freundlich equation, which is more precise at low concentration range than Langmuir equation. Literature study on the adsorption systems of dyes and phenols was done to verify the large adsorbent savings in countercurrent two- and three-adsorption processes. In this study, activated carbon derived from plum kernels, an agricultural waste product was prepared using KOH activation. Isotherm adsorption of dyes and phenols were investigated and analyzed with the Freundlich equation proving the superiority of countercurrent two- and three-stage adsorption processes and determining the optimum number of operating stages for engineering applications.

2. Materials and method

2.1. Preparation of the activated carbon

Activated carbon was prepared from plum kernels using carbonization and activation, a two-step process. During carbonization, the oven temperature was kept at 450 °C for 1.5 h. In the

* Corresponding author. Tel.: +886 37 381575; fax: +886 37 332397.
E-mail address: wfc@nuu.edu.tw (F.-C. Wu).

0304-3894/$ – see front matter © 2008 Published by Elsevier B.V.
doi:10.1016/j.jhazmat.2008.05.031

Nomenclature

C_e	liquid-phase concentration at equilibrium (g/m^3)
C_i, C_f	initial and final solute concentration in the aqueous phase (mol/m^3)
K_L	Langmuir constant defined in Eq. (19) (m^3/g)
K_F	Freundlich constant defined in Eq. (3) (g/kg)(g/m^3)^n
K'_F	Freundlich constant defined in Eq. (4) (kg/m^3)^n
m_{y_i}, m_{y_f}	initial and final solute mass flow rate (kg/s)
m_{x_0}, m_{x_1}	influent and effluent adsorbent mass flow rate of first tank (kg/s)
m_{x_s}, m_{x_d}, m_{x_t}	mass flow rate of single, two- and three-stage adsorbent (kg/s)
q_e	amount of adsorption at equilibrium (g/kg)
q_{mon}	amount of adsorption corresponding to monolayer coverage (g/kg)
x_0, x_f	the starting and final solute quotient in adsorbent
y_i, y_f	the starting and final solute quotient in solution
ρ	solution density (kg/m^3)

meantime, nitrogen gas was flowed into the oven at a rate of 3 dm^3/min.

During activation, the mixture of water/KOH/char ratio equal to 1/1/1 by mass was placed in a sealed ceramic oven, heated at a rate of 10 °C/min to 780 °C, and kept at this temperature for 1 h. The samples were classified according to KOH/char rate of 0, 0.5, 1.0, 2.0, 3.0, 4.0, and 5.0 and denoted as PKKC00, PKKC05, PKKC10, PKKC20, PKKC30, PKKC40, and PKKC50, respectively.

2.2. Procedures for adsorption experiments

A commercial-grade acid Blue 74 (AB74, M_W (molecular weight) = 466.4 g/mole) and basic brown 1 (BB1, M_W = 419.4 g/mole), were used. The methylene blue (MB, M_W = 284.3 g/mole), phenol (M_W = 94 g/mole), and 4-chlorophenol (4-CP, M_W = 128.5 g/mole) were analytical reagent grade. The molecular weight of the MB did not include the associated chloride ion. The procedures for the adsorption equilibrium experiments were the same as those in a previous study [17].

3. Results and discussion

3.1. Superior countercurrent two- and three-stage adsorption systems

The single-stage adsorption operation is shown in Fig. 1(a). Suppose that the solid and the liquid are completely separated, then solution mass flow rate is constant ($m_{y_i} = m_{y_f} = m_y$) and adosorbent mass flow rate is constant ($m_{x_0} = m_{x_1} = m_x$). The starting and final solute quotients in solution in single-stage adsorption are, respectively, y_i and y_f; the starting and final solute quotients in adsorbent are, respectively, x_0 and x_f. In adsorption operation process, solute decrease in solution is equal to solute increase in adsorbent; the mass balance for the solute is

$$m_y(y_i - y_f) = m_x(x_f - x_0) \tag{1}$$

$$\left(\frac{m_x}{m_y}\right)_s = \frac{y_i - y_f}{x_f - x_0} \tag{2}$$

Suppose the adsorption equilibrium is described with the Freundlich isotherm equation, then

$$q_e = K_F C_e^{1/n} \tag{3}$$

When, in Eq. (3), the solute concentration C_e in the solution is replaced with y_j and the solute concentration (adsorption amount) q_e in the solid phase (adsorbent) is replaced with x_j, the Freundlich constant K_F in solution is replaced with K'_F, and ρ is the solution mass per unit volume of the solution, then the Freundlich isotherm equilibrium of the jth stage (jth = 1, 2, 3, . . ., any one stage) rewrite is

$$x_j = K'_F \varrho^{1/n} y_j^{1/n} \tag{4}$$

The solute equilibrium relationship between the solid and the liquid phase of adsorption described with Eq. (4) is called the isotherm curve.

If fresh adsorbent is used, then $x_0 = 0$, and the isotherm curve of Eq. (4) (at single-stage $x_1 = x_f$, $y_1 = y_f$, see Fig. 1(a)) is inserted into Eq. (2), then obtain

$$\left(\frac{m_x}{m_y}\right)_s = \frac{y_i - y_f}{K'_F \varrho^{1/n} y_f^{1/n}} \tag{5}$$

If Freundlich constant is known, the mass ratio $(m_x/m_y)_s$ of adsorbent to solvent for the single-stage can be calculated from Eq. (5).

Fig. 1(b) shows the analysis of the countercurrent two-stage adsorption operation. Suppose $m_{y_i} = m_{y_2} = m_{y_f} = m_y$, $m_{x_0} = m_{x_1} = m_{x_2} = m_x$. Doing a mass balance for the solute, then

$$\left(\frac{m_x}{m_y}\right)_d = \frac{y_2 - y_f}{x_1 - x_0} = \frac{y_i - y_2}{x_2 - x_1} = \frac{y_i - y_f}{x_2 - x_0} \tag{6}$$

$$\left(\frac{m_x}{m_y}\right)_d = \frac{y_2 - y_f}{K'_F \varrho^{1/n}\, y_f^{1/n}} \tag{7}$$

If $x_0 = 0$, and isotherm curve is expressed with Freundlich equation, then obtain

$$\frac{y_2 - y_f}{K'_F \varrho^{1/n} y_f^{1/n}} = \frac{y_i - y_f}{K'_F \varrho^{1/n} y_2^{1/n}} \tag{8}$$

After rearrangement, obtain

$$\frac{y_2 - y_f}{y_i - y_f} = \left(\frac{y_f}{y_2}\right)^{1/n} \tag{9}$$

When y_i, y_f, and Freundlich constant are known, middle concentration y_2 of countercurrent two-stage systems can be calculated from Eq. (9).

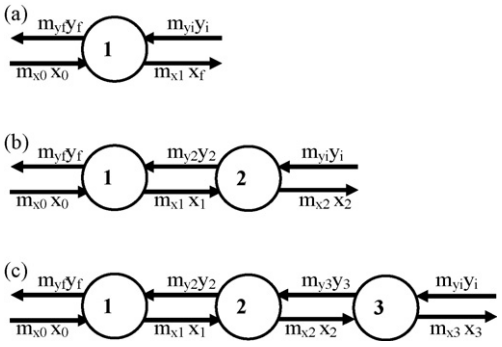

Fig. 1. Adsorption processes: (a) single-stage; (b) countercurrent two-stage; (c) countercurrent three-stage.

The adsorbent mass ratio of the countercurrent two-stage to the single-stage system can be obtained from Eq. (10), which is obtained by dividing Eq. (7) by Eq. (5).

$$\frac{(m_x/m_y)_s}{(m_x/m_y)_d} = \frac{y_i - y_f}{y_2 - y_f} = \frac{m_{x_s}}{m_{x_d}} \tag{10}$$

where m_{x_s}/m_{x_d} is the adsorbent mass ratio of the countercurrent two-stage to the single-stage system. Let $y_f/y_i = 0.01$, calculation results of Eqs. (9) and (10) for various $1/n$ values are listed in Table 1. Table 1 shows that the m_{x_s}/m_{x_d} value increases rapidly with increased $1/n$ value, and the higher the $1/n$ value of the adsorption system the lower the adsorbent consumption with the countercurrent two-stage system.

The countercurrent three-stage adsorption operation is shown in Fig. 1(c). Suppose $m_{y_i} = m_{y_2} = m_{y_3} = m_{y_f} = m_y$, $m_{x_0} = m_{x_1} = m_{x_2} = m_{x_3} = m_x$. Doing mass balance for the solute, then

$$\left(\frac{m_x}{m_y}\right)_t = \frac{y_2 - y_f}{x_1 - x_0} = \frac{y_3 - y_f}{x_2 - x_0} = \frac{y_i - y_f}{x_3 - x_0} \tag{11}$$

$$\left(\frac{m_x}{m_y}\right)_t = \frac{y_2 - y_f}{K'_F \varrho^{1/n} y_f^{1/n}} \tag{12}$$

If $x_0 = 0$, then

$$\frac{y_2 - y_f}{x_1} = \frac{y_3 - y_f}{x_2} \tag{13}$$

$$\frac{y_2 - y_f}{x_1} = \frac{y_i - y_f}{x_3} \tag{14}$$

When the isotherm curve follows the Freundlich equation, Eqs. (13) and (14) can be rearranged, respectively, as

$$\frac{y_2 - y_f}{y_3 - y_f} = \left(\frac{y_f}{y_2}\right)^{1/n} \tag{15}$$

$$\frac{y_2 - y_f}{y_i - y_f} = \left(\frac{y_f}{y_3}\right)^{1/n} \tag{16}$$

When y_i, y_f, and the Freundlich constant are known, the middle concentration (y_2 and y_3) of countercurrent three-stages can be obtained by simultaneously solving Eqs. (15) and (16). The adsorbent mass ratio of the countercurrent three-stage to the single-stage can be obtained from Eq. (17), which is obtained by dividing Eq. (12) by Eq. (5). Let solution mass flow rate be constant ($(m_y)_s = (m_y)_t$).

$$\frac{(m_x/m_y)_s}{(m_x/m_y)_t} = \frac{y_i - y_f}{y_2 - y_f} = \frac{m_{x_s}}{m_{x_t}} \tag{17}$$

where m_{x_s}/m_{x_t} is the adsorbent mass ratio of the countercurrent three-stages to the single-stage. Let $y_f/y_i = 0.01$. Calculation results of Eqs. (15)–(17) for various $1/n$ values are listed in Table 1. The tendency of the m_{x_s}/m_{x_t} value to increase with an increased $1/n$ value to higher than the m_{x_s}/m_{x_d} value is more significant at a higher $1/n$ value. This means that a better adsorbent consumption reduction is obtained at higher $1/n$ value in the countercurrent three-stage system. Furthermore, the m_{x_d}/m_{x_t} values obtained by dividing m_{x_s}/m_{x_d} by m_{x_s}/m_{x_t} are listed in Table 1 for judging the optimum number of stages.

Table 1
Ratio of adsorbent consumption between single-stage, countercurrent two-stage and countercurrent three-stage process and the optimum number of stages of countercurrent multi-stage systems (at $y_f/y_i = 0.01$)

$1/n$	m_{x_s}/m_{x_d}	m_{x_s}/m_{x_t}	m_{x_d}/m_{x_t}	Optimum stage number
0.01	1.047	1.047	1.000	Single
0.03	1.143	1.148	1.004	Single
0.06	1.297	1.318	1.016	Two
0.1	1.521	1.582	1.040	Two
0.2	2.158	2.440	1.131	Two
0.3	2.908	3.649	1.255	Three
0.5	4.699	7.280	1.549	Three
0.6	5.721	9.724	1.700	Three
0.8	7.974	15.82	1.984	Three
1.0	10.46	23.30	2.228	Three or >three

Let $y_f/y_i = 0.01$. The relationship between the calculated values of ratios of adsorbent consumption, m_{x_s}/m_{x_d}, m_{x_s}/m_{x_t} and m_{x_d}/m_{x_t}, and $1/n$ values are plotted as in Fig. 2. Fig. 2 shows that at a higher $1/n$ value, tremendous adsorbent consumption reduction can be obtained by converting the single-stage system into countercurrent two- and three-stage systems. If the ratio of the adsorbent consumption is larger than 1.25, then the stage increase is economically feasible. The horizontal line of ratio of the adsorbent consumption is equal to 1.25 intersects with curves of m_{x_s}/m_{x_d} and m_{x_d}/m_{x_t} at $1/n$ values of 0.05 and 0.3, respectively. This means that when $1/n \leq 0.05$, then the single-stage system is suitable; when $0.05 < 1/n \leq 0.3$, then the countercurrent two-stage system is suitable; and when $1/n > 0.3$, then the countercurrent three-stage system is feasible.

3.2. Design and operation of the countercurrent three-stage adsorption system

The designed continuous-flow countercurrent three-stage adsorption system is shown in Fig. 3. It shows that the liquid flows by gravitation. V1, V2, and V3 are upright tanks with different volumes and heights. The slope of all the tank bottoms is 1/12, making it possible for solid particles to be easily discharged to the next stage tank. The required volumes of the tanks are calculated from the retention time. Let the width ratio be V1, V2, and V3 = 3:4:5 and the heights of the three thanks are calculated accordingly. When the ratio of height to width of the tank is larger than 1.5, another set of impellers is added. The operation mode is as follows:

Liquid: the liquid continuously flows into V3 at a flow rate m_{y_i}, comes into complete contact with the adsorbent, and overflows into V2. The overflow opening is covered with a screen to keep the adsorbent from being washed away. The liquid flows into and out of V2 and V1 as does it into and out of V3.

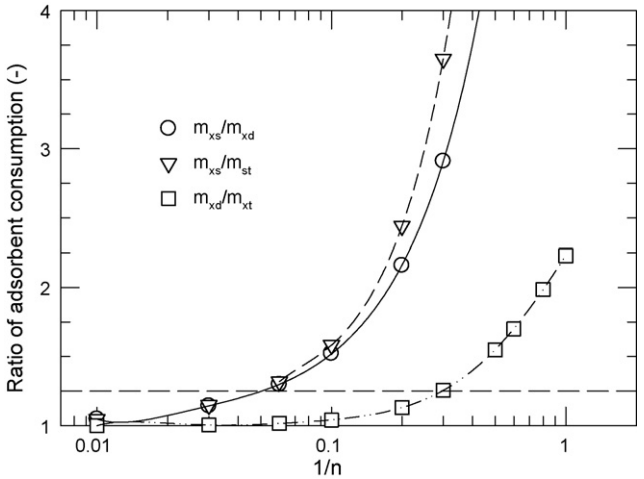

Fig. 2. The effect of $1/n$ value on the adsorbent consumption for 2- and 3-stage countercurrent processes.

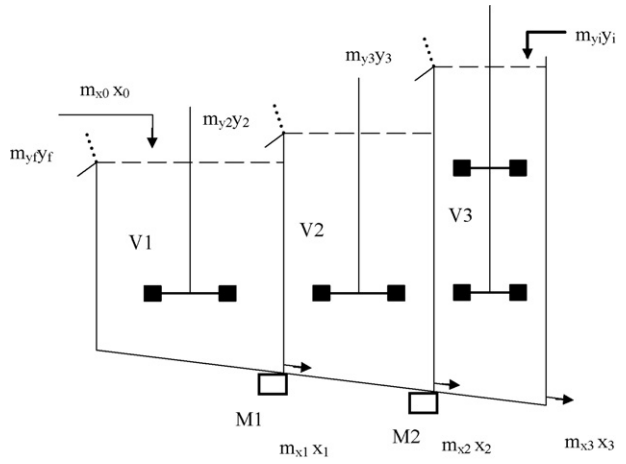

Fig. 3. Design of a continuous-flow countercurrent three-stage adsorption system.

Adsorbent: The virgin adsorbent continuously enters V1 at a flow rate of m_{x_0}, is stirred and comes into complete contact with the liquid, and adsorbs the solute in the solution. After the retention time is over, the adsorbent is transferred to tank V2 via a slanted tank bottom with a gear pump. Because the liquid level of V2 is higher than that of V1, power is needed to transfer the settled adsorbent slurry. The function of the adsorbent in V2 and V3 is the same as in V1.

Notes for design: (1) The agitating speed of the stirrer should be fast enough for complete mixing, but not so fast as to the break adsorbent up. (2) If the adsorbent particles are small or their specific gravity is close to that of the liquid, M1 and M2 are converted into continuous centrifugal thickeners. The supernatant is recycled and the thickened slurry goes to the next tank. (3) For offsetting a small side flow and insufficient contact time, inevitable differences between the quantities of actual measurements and those of theoretical calculation, 5–10% extra adsorbent is added. (4) If the $1/n$ value is between 0.05 and 0.3 and the countercurrent two-stage system is adopted, this design mode is still applicable; in this case, only two tanks are needed.

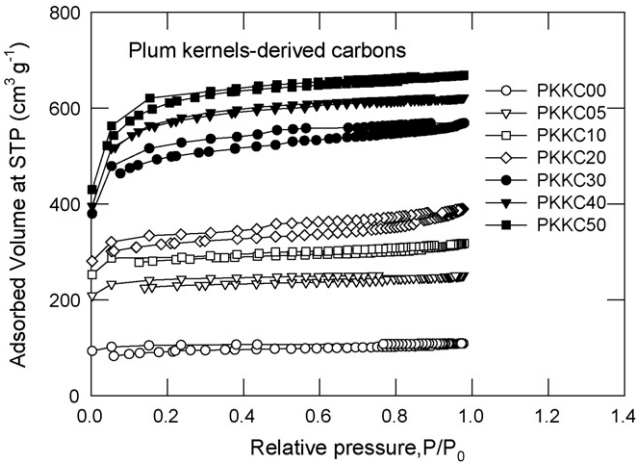

Fig. 4. Adsorption/desorption isotherms of N_2 at 77 K on steam-activated carbons derived from plum kernels (carbons are: PKKC00 (○), PKKC05 (▽), PKKC10 (□), PKKC20 (◊), PKKC30 (●), PKKC40 (▼), and PKKC50 (■)).

3.3. 1/n values of the Freundlich equation

Table 2 lists the parameter values of the Freundlich equation for 57 adsorption systems of dyes on various kinds of adsorbents collected from literature. They are in ascending order of $1/n$ values. As mentioned before, the $1/n$ values are classified into three regions according to the optimum number of stages necessary for the countercurrent adsorption systems. When $1/n \leq 0.05$, a single-stage system is adopted; none of those listed in Table 2 is in this region. Thirty nine (39) systems (68%) in the list are in the region of $0.05 < 1/n \leq 0.3$ being suitable for a countercurrent two-stage system. Eighteen (18) systems (32%) are in the region of $0.3 < 1/n \leq 1.0$ being suitable for a countercurrent three-stage system.

Furthermore, Table 3 lists the parameter values of the Freundlich equation for 53 adsorption systems of phenols on various kinds of adsorbents collected from literature. Table 3 shows that none of

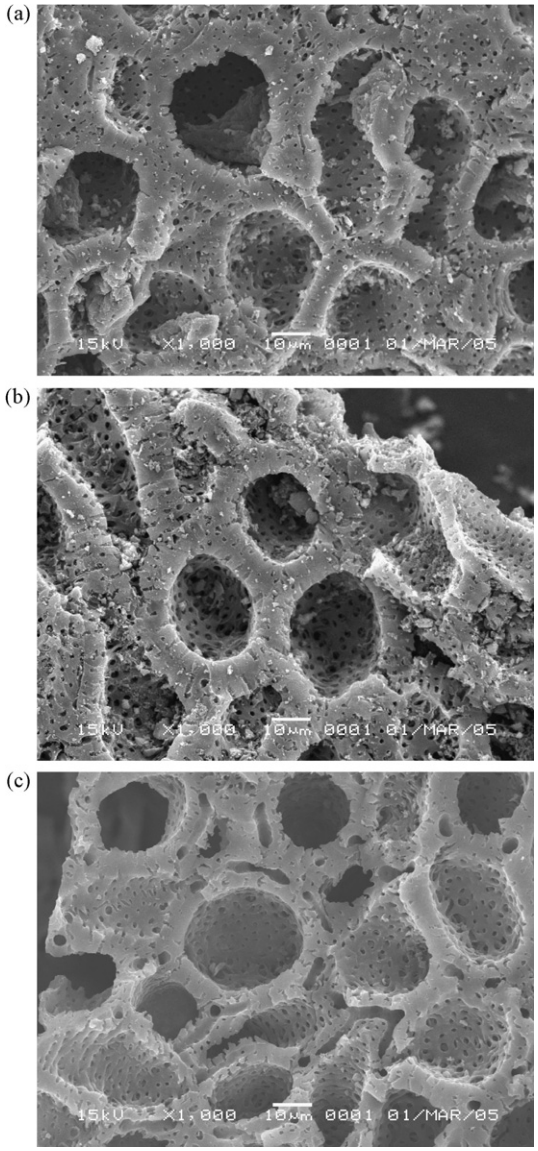

Fig. 5. SEM photos: (a) PKKC00, (b) PKKC20, and (c) PKKC50.

Table 2
Freundlich parameters $1/n$ and K_F for dyes collected from literature

No.	$1/n$	Adsorbent	Adsorbate	K_F[a]	Reference
1	0.056	AC: 180–250 μm	MB (pH 7)	178	[22]
2	0.077	AC < 106 μm	MB (pH 4)	183	[22]
3	0.077	AC4	Basic dye	490	[23]
4	0.096	PKSAC	BB9	195	[24]
5	0.098	Bio-plant AC	MB	71.6	[25]
6	0.101	CSAC	Bismark brown R	598	[26]
7	0.102	AC4	Acid dye	177	[27]
8	0.103	AC < 106 μm	MB (pH 7)	185	[22]
9	0.108	AC	Telon blue (AB25)	110	[28]
10	0.111	CZ300	MB	284	[29]
11	0.117	SAC	Bismark brown R	1003	[26]
12	0.123	GAC	MG-400	77.8	[30]
13	0.129	CB-100 (AC)	Acid orange 10	3.20	[31]
14	0.129	CPAC	Malachite green	143	[32]
15	0.137	F100	MB	123	[29]
16	0.145	AC	Deorlene yellow	112	[22]
17	0.147	CS600	MB	40	[33]
18	0.150	CC-15 (AC)	AB80	179	[34]
19	0.150	CZ300	Erythrosine red	262	[29]
20	0.161	F400	RY	67.7	[35]
21	0.175	$CP55_{OX}$	MB	199	[36]
22	0.183	S800/30	MB	0.66[b]	[37]
23	0.193	AC cloth	AB120	3.7E−4[b]	[38]
24	0.195	GSPAC	Malachite green	128	[32]
25	0.199	Sawdust (AC)	Direct blue 2B	202	[39]
26	0.200	AC	Disperse blue	2.8	[28]
27	0.204	SDC (AC)	AY36	41.7	[40]
28	0.204	AC4	Reactivate dye	71	[27]
29	0.208	F400	RN	19.6	[35]
30	0.210	Commercial (ACC)	Basic yellow	3.49	[41]
31	0.212	AC cloth	AB92	6.8E−4[b]	[38]
32	0.213	CP55	MB	72	[33]
33	0.217	F400	RR	20.0	[35]
34	0.225	PAC (Merck)	BV10	71.3	[42]
35	0.233	ACH	MB	3.31	[43]
36	0.244	$CS600_{OX}$	MB	41	[36]
37	0.251	Sawdust (AC)	Direct green B	88.3	[39]
38	0.256	$K700_{OX}$ (AC)	MB	89.0	[44]
39	0.256	AC cloth	AB129	1.9E−3[b]	[38]
40	0.318	F100	Erythrosine red	11	[29]
41	0.322	AC cloth	AB45	4.9E-3[b]	[38]
42	0.323	AC	Victoria blue	3.1	[28]
43	0.326	CAC	Bismark brown R	54	[26]
44	0.346	Commercial (ACC)	Acid blue	2.27	[41]
45	0.391	Coffee grounds (ACP)	Basic yellow	2.04	[41]
46	0.411	ACC	Malachite green	1.19	[45]
47	0.435	RHC (AC)	AY36	2.1	[40]
48	0.435	Rice husk (AC)	Acid yellow 36	2.1[b]	[46]
49	0.441	Wheat shells	Direct blue 71	8.14	[47]
50	0.446	Wheat bran	Astrazon Yellow 7GL	1.55	[48]
51	0.449	ACL	Malachite green	5.63	[45]
52	0.469	PAC (Merck)	BV3	17.1	[42]
53	0.511	PAC (Merck)	BB1	23.8	[42]
54	0.524	PAC (Merck)	BR9	5.9	[42]
55	0.556	ACA	MB	0.10	[43]
56	0.589	PAC (Merck)	Reactive black 5	5.75	[49]
57	0.714	Coffee grounds (ACP)	AB25	2.27	[41]

[a] K_F: $((g/kg)(g/m^3)^n)$.
[b] K_F: $((mmol/kg)(g/m^3)^n)$.

$1/n$ values is less than 0.05; 23 systems (43%) are in the region $0.05 < 1/n \leq 0.3$; 30 systems (57%), $0.3 < 1/n \leq 1.0$.

According to the above $1/n$ values collected from literature, almost all the adsorption systems are suitable for economical operations of countercurrent two- or three-stage systems.

3.4. Properties of the activated carbons

Before designing and using the adsorption process, the pore structure of the adsorbent must be determined [18,19]. Fig. 4 shows the curves of the 77 K N_2 isotherm adsorption/desorption of the activated carbon obtained at 7 different values of the KOH/char ratio in this study. Values of KOH/char ratio of group 1 activated carbon were from 0 to 2 (empty circles in the figure); those of group 2 were from 3 to 5 (solid circles in the figure). Fig. 4 shows that the adsorption volume of group 1 activated carbons did not significantly change when the values of P/P_0 were increased from minimum to maximum, the pores being mostly straight tubes [20]. The adsorption volume of this type of activated carbon was low. For group 2 activated carbons, when P/P_0 to the limit to zero the adsorption volumes of PKK30, PKK40 and PKK50 were closer to 381–430 cm^3/g The adsorption volumes of these three activated

Table 3
Freundlich parameters $1/n$ and K_F for phenols collected from literature

No.	$1/n$	Adsorbent	Adsorbate	K_F[a]	Reference
1	0.094	t_A4.0	*o*-Cresol	209	[17]
2	0.130	GAC(oxic)	*o*-Cresol	190	[50]
3	0.138	Calgon F-1400	4-NP	254	[51]
4	0.140	Commercial (ACC)	Phenol	2.41	[41]
5	0.141	Calgon F-1400	4-CP	331	[51]
6	0.150	GAC(oxic)	Nitrophenol	87.0	[50]
7	0.187	Pistachio (steam AC)	Phenol	87.3	[52]
8	0.195	Norit SA4 (PAC)	2-CP	86.5	[53]
9	0.202	SP207A	4-CP	1.46[b]	[54]
10	0.223	Calgon F-1400	Phenol	198	[51]
11	0.227	Norit PKDA (GAC)	2-CP	60.4	[53]
12	0.230	APET carbons	Phenol (unbuffered)	2.2[b]	[55]
13	0.236	CZ300	Phenol	73	[29]
14	0.237	Fir wood (steam AC)	Phenol	21.1	[52]
15	0.238	ACH	Phenol	41.3	[43]
16	0.240	CZ52942	Phenol	96	[56]
17	0.245	SP207A	Phenol	0.95[b]	[54]
18	0.256	t_A4.0	Phenol	53.5	[17]
19	0.259	208C	4-CP	2.12[b]	[54]
20	0.260	F-300	2-NP	101	[57]
21	0.263	Activated 850/5	Phenol	1.12	[58]
22	0.265	t_A4.0	3-CP	95.6	[17]
23	0.278	208C	Phenol	1.21[b]	[54]
24	0.303	F100	Phenol	44	[29]
25	0.309	RGM1 (GAC)	4-CP	28.8	[59]
26	0.310	F400	Phenol	39	[56]
27	0.312	S800/30	Phenol	0.97[b]	[37]
28	0.319	F400	Phenol	36.3	[60]
29	0.320	CSAC	4-CP	9.21	[61]
30	0.355	S800/30	4-NP	0.81[b]	[37]
31	0.357	ACA	Phenol	7.13	[43]
32	0.370	Coffee grounds (ACP)	Phenol	1.07	[41]
33	0.378	CAC	4-CP	9.11	[61]
34	0.380	BESTCHEM (AC)	Phenol	15.7	[62]
35	0.396	RGM1 (GAC)	Phenol	0.851	[37]
36	0.398	Pica 103	4-CP	1.73[b]	[56]
37	0.410	Sludge derived (AC)	Phenol	2.69	[62]
38	0.410	F-300	2-CP	51	[57]
39	0.420	Sigma-AC	Phenol	37.0	[60]
40	0.436	Pica 103	Phenol	0.77[b]	[54]
41	0.450	ACF	2,4-DCP	61.4	[63]
42	0.517	RGM1 (GAC)	2,4,6-TCP	13.37	[59]
43	0.534	RGM1 (GAC)	4-CP	3.034	[59]
44	0.540	F-300	Phenol	21	[57]
45	0.547	RGM1 (GAC)	2,4-DCP	6.934	[59]
46	0.602	CAC	2,4,6-TCP	2.94	[61]
47	0.616	GAC	Phenol	6.19	[64]
48	0.681	CSAC	2,4,6-TCP	2.05	[61]
49	0.683	CWZ30 (PAC)	Phenol	70.2	[65]
50	0.769	RSCC	Phenol	15.5	[66]
51	0.788	UMC (AC)	Phenol	2.53	[67]
52	0.822	WVA1100 (AC)	Phenol	1.76	[67]
53	0.870	IIT carbon	Phenol	0.44	[68]

[a] K_F: $((g/kg)(g/m^3)^n)$.
[b] K_F: $((mmol/kg)(g/m^3)^n)$.

Table 4
Physical properties of carbons derived from plum kernels with KOH activation

Carbons	S_p (m^2/g)	S_{micro}/S_p	V_{pore} (cm^3/g)	V_{micro}/V_{pore}	D_p (nm)	ρ_b (kg/m^3)
PKKC00	290	0.903	0.169	0.766	2.3	
PKKC05	644	0.946	0.388	0.871	2.4	457
PKKC10	784	0.938	0.491	0.845	2.5	348
PKKC20	971	0.885	0.601	0.718	2.5	355
PKKC30	1495	0.917	0.877	0.811	2.3	164
PKKC40	1725	0.938	0.959	0.867	2.2	121
PKKC50	1901	0.924	1.030	0.837	2.2	140

carbons increased rapidly when P/P_0 was first increased, then increased less, and then increased least after $P/P_0 > 0.2$. The tendencies of these three curves are similar; i.e. they have similar pore size distributions.

Table 4 lists BET surface area related data (S_p, S_{micro}/S_p, V_{pore}, V_{micro}/V_{pore}, and D_p) obtained from 77 K N_2 isotherm adsorption with a sorptiometer. Among them, surface area (S_p) and pore volume (V_{pore}) increased with increased KOH/char value;

Table 5
Parameters of the Langmuir and Freundlich equations with the adsorption of dyes at 30 °C onto the activated carbons prepared from plum kernels

Solute	Activated carbon	Langmuir equation				Freundlich equation			
		q_{mon} (g/kg)	K_L (m^2/g)	r^2	Δq%	1/n (−)	K_F^*	r^2	Δq%
MB	PKKC10	372	0.0313	0.980	18.7	0.148	138.9	0.958	5.07
	PKKC20	481	0.0748	0.996	17.7	0.148	198.3	0.988	3.13
	PKKC30	757	0.2367	0.999	20.1	0.116	403.6	0.974	4.15
	PKKC40	941	0.8389	1.000	16.1	0.039	767.5	0.993	0.67
BB1	PKKC10	622	0.0456	0.999	7.59	0.199	178.5	0.965	7.31
	PKKC20	797	0.0469	0.996	4.95	0.209	219.4	0.971	9.01
	PKKC30	1082	0.0559	0.996	8.04	0.247	255.7	0.983	5.49
	PKKC40	1405	0.1029	0.996	12.2	0.231	404.9	0.988	7.24
AB74	PKKC10	127	0.0271	0.992	5.28	0.249	27.89	0.986	1.90
	PKKC20	229	0.0597	0.998	7.31	0.241	59.47	0.979	4.28
	PKKC30	314	0.0692	0.989	9.58	0.216	94.74	0.987	2.32
	PKKC40	388	0.1118	0.996	14.3	0.160	162.9	0.996	1.26

K_F^* : ((g/kg)(g/m^3)^n).

Table 6
Parameters of the Langmuir and Freundlich equations with the adsorption of phenols at 30 °C onto the activated carbons prepared from plum kernels

Solute	Activated carbon	Langmuir equation				Freundlich equation			
		q_{mon} (g/kg)	K_L (m^2/g)	r^2	Δq%	1/n (−)	K_F^*	r^2	Δq%
Phenol	PKKC10	185	0.0268	0.995	5.05	0.275	34.99	0.979	2.98
	PKKC20	202	0.0312	0.995	6.81	0.246	45.49	0.992	2.16
	PKKC30	253	0.0340	0.995	6.98	0.270	51.38	0.987	3.28
	PKKC40	309	0.0540	0.996	9.23	0.250	74.77	0.980	4.43
4-	PKKC10	335	0.0320	0.995	5.08	0.231	80.09	0.982	3.47
CP	PKKC20	395	0.0509	0.996	8.51	0.225	104.3	0.951	6.44
	PKKC30	455	0.0711	0.997	13.9	0.195	146.7	0.967	5.53
	PKKC40	582	0.0926	0.997	14.9	0.218	174.5	0.971	6.82
2,4-	PKKC10	383	0.0369	0.996	14.8	0.135	156.2	0.997	1.06
DCP	PKKC20	512	0.0545	0.996	15.3	0.159	191.4	0.986	3.10
	PKKC30	586	0.1469	0.991	18.0	0.158	227.4	0.983	3.64
	PKKC40	759	0.2248	1.000	13.4	0.059	533.9	0.997	0.65

K_F^* : ((g/kg)(g/m^3)^n).

Table 7
Adsorbent consumption ratios of PKKC30 in the countercurrent single-, two-, three-stage systems

	Solutes	MB	BB1	AB74	Phenol	4-CP	2,4-DCP
Basic	K_F	403.6	255.7	94.74	51.38	146.7	227.4
Data	1/n	0.116	0.247	0.216	0.270	0.195	0.158
Operation	C_i (g/m^3)	700	1000	400	470.5	643	815.5
Condition	C_f (g/m^3)	7.0	10.0	4.0	4.7	6.4	8.2
Single-stage	m_{x_s} (kg/m^3)	1.37	2.19	3.10	5.97	3.02	2.55
Two-	m_{x_d} (kg/m^3)	0.848	0.877	1.36	2.23	1.42	1.36
stage	C_2 (g/m^3)	436	407	178	179	305	441
Three-	m_{x_t} (kg/m^3)	0.808	0.739	1.19	1.84	1.26	1.25
stage	C_2 (g/m^3)	416	344	156	148	270	406
	C_3 (g/m^3)	663	811	339	368	556	746

micropore area ratio (S_{micro}/S_p) and micropore volume ratio (V_{micro}/V_{pore}) were not affected by the changed KOH/char values, the activated carbon having a higher micropore ratio; sizes of average pore diameters (D_p) are concentrated in the range of 2.2–2.5 nm.

Fig. 5(a)–(c) are 1000× magnified SEM photos of the activated carbons. Fig. 5(a) shows that PKKC00 was under physical activation, the main reaction being on surface pore walls. The surface of pore walls appeared gray white caused by the activation reaction. Fig. 5(b) shows that PKKC20 was under both chemical and physical activation. Activation took place on the outside surface of the walls and the interiors of the pores, thus, the gray white gradually spread to the middle of the pore walls. Fig. 5(c) shows that PKKC50 was mainly under chemical activation. The whole material was activated uniformly, thus, the gray white spread uniformly over the whole material.

3.5. Adsorption equilibrium and isotherm equation

Three dyes (MB, AB74 and MB) and three phenols (phenol, 4-CP and 2,4-DCP) were used as adsorbates and PKKC10, PKKC20, PKKC30, and PKKC40, activated carbons of different KOH/char ratio, were used as adsorbents for the isotherm equilibrium adsorption study. The results are shown in Fig. 6 (a)–(f) and Table 6 discussed later. The Langmuir and Freundlich isotherm equations were used for analysis.

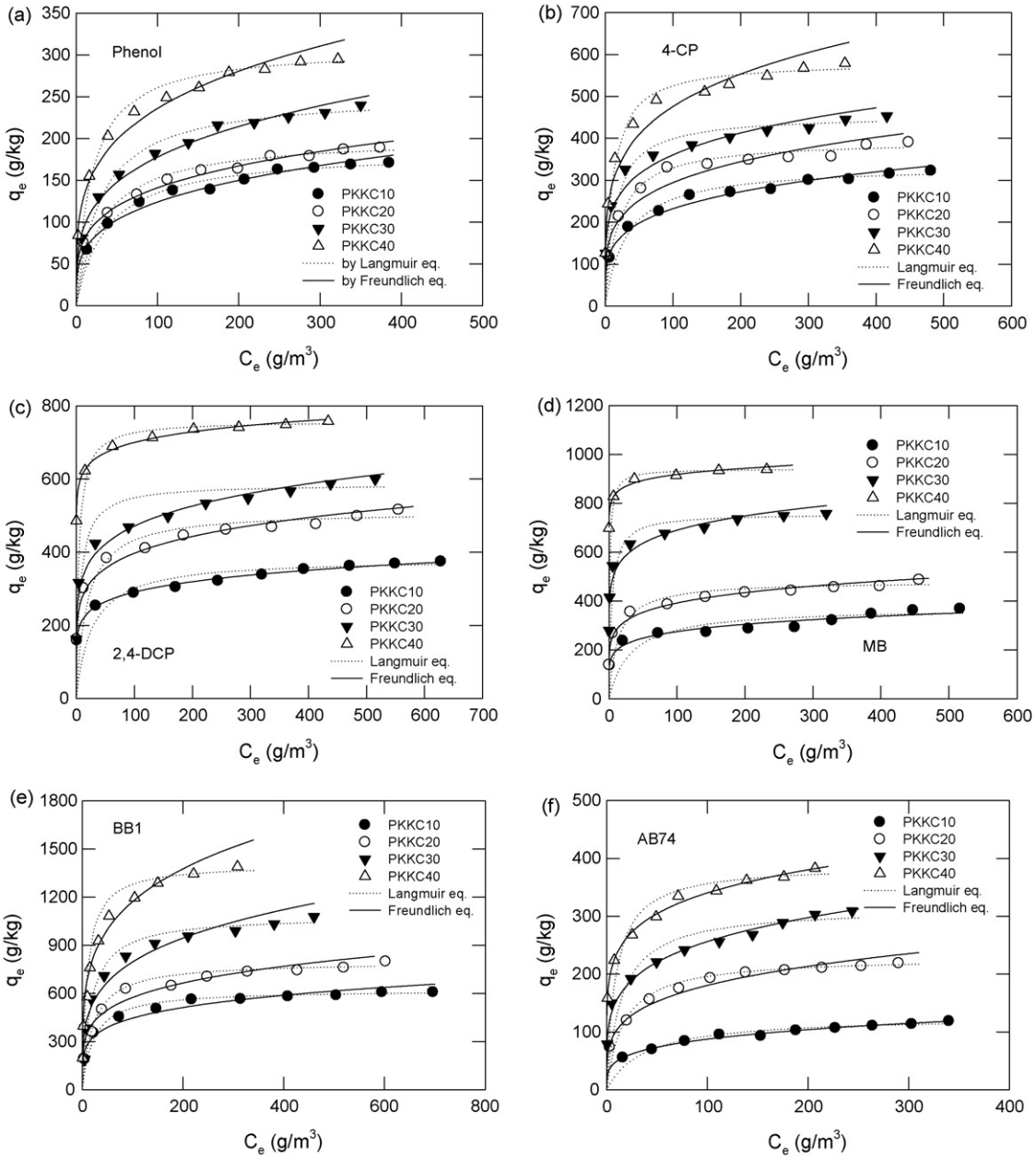

Fig. 6. Adsorption isotherm of phenol, 4-CP, 2,4-DCP, MB, BB1, and AB74 on KOH-activated carbon derived from plum kernels (carbons are: PKKC10 (●), PKKC20 (○), PKKC30 (▼), and PKKC40 (□) respectively; Freundlich equation (—) and Langmuir equation (···)).

In order to compare the validity of two isotherm equations, a normalized standard deviation Δq_e (%) is calculated,

$$\Delta q_e(\%) = 100\sqrt{\frac{\sum[(q_{e,exp} - q_{e,cal})/q_{e,exp}]^2}{(N-1)}} \quad (18)$$

where N is the number of data points.

The Langmuir equation is as follow:

$$\frac{C_e}{q_e} = \frac{1}{K_L q_{mon}} + \left(\frac{1}{q_{mon}}\right) C_e \quad (19)$$

where q_{mon} is the amount of adsorption (in g/kg) corresponding to complete monolayer coverage and K_L is the Langmuir constant. If C_e/q_e is on the Y-axis and C_e is on the X-axis, the slope $(1/q_{mon})$ and intercept $(1/K_L q_{mon})$ can be obtained from the procedures of least squares and correlation coefficient (r^2) can also be obtained from the data. Table 5 lists the q_{mon}, K_L, r^2 and $\Delta q\%$ values. The r^2 is between 0.980 and 1.000, seemingly a good equation fitting; $\Delta q\%$ values are high at the interval of 4.95 and 20.1%. The Freundlich equation is as follow:

$$\ln q_e = \ln K_F + \left(\frac{1}{n}\right) \ln C_e \quad (20)$$

If $\ln q_e$ is on the Y-axis and $\ln C_e$ is on the X-axis, the slope $(1/n)$ and intercept $(\ln K_F)$ can be obtained from the procedures of least squares and correlation coefficient (r^2) and percent standard deviation ($\Delta q\%$) can also be obtained from the data. Table 5 lists the $1/n$, K_F, r^2 and $\Delta q\%$ values of the Freundlich equation. When r^2 values are compared, those of Freundlich equation are between 0.958 and 0.996, lower than Langmuir equation are between 0.980 and 1.000. When $\Delta q\%$ values are compared, those of Freundlich equation are between 0.67 and 5.49%, superior to those of Langmuir equation

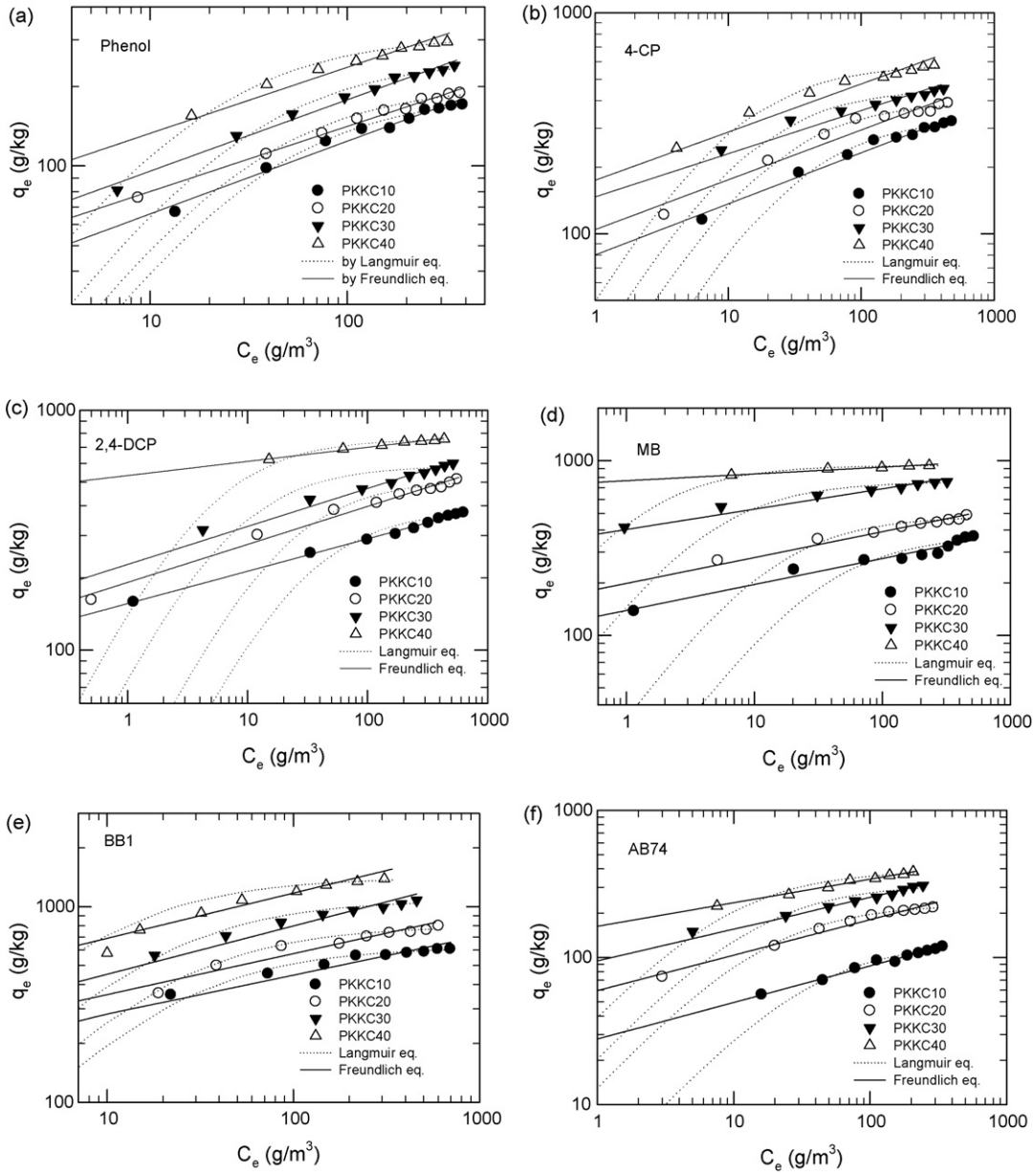

Fig. 7. Adsorption isotherm equilibrium of phenol, 4-CP, 2,4-DCP, MB, BB1, and AB74 on KOH-activated carbon derived from plum kernel at low concentration range (carbons are: PKKC10 (●), PKKC20 (○), PKKC30 (▼), and PKKC40 (□), respectively; Freundlich equation (—) and Langmuir equation (···)).

which are between 4.94 and 18.7%. Based on $\Delta q\%$ values, the Freundlich equation appears better fitted. Only one of $1/n$ values of 12 adsorption systems of three dyes on activated carbons of this study is smaller than 0.05, the others being in the range of 0.05–0.3, which is suitable for a countercurrent two-stage system.

Table 6 shows the $\Delta q\%$ values of the Langmuir equation of phenols are between 5.05 and 18%, while those of the Freundlich equation are between 0.65 and 6.82%, thus, the Freundlich equation is better fitted. The values of $1/n$ of the 12 adsorption systems for phenols are between 0.05 and 0.3, suitable for a countercurrent two-stage system.

As mentioned above, the r^2 values based on the Langmuir equation were closer to 1.0 than those based on the Freundlich equation, while the values of standard deviation $\Delta q\%$ based on Freundlich equation were lower. Fig. 6 shows two curves obtained from the Freundlich equation (solid line) and Langmuir equation (dotted line), together with experimental data of the adsorption systems. It not easy to differentiate which equation is better fitted to the data. Fig. 7 is a log–log scale coordinate, showing better fitting for the Freundlich equation at low concentration range but poor fitting for the Langmuir equation at the same range of concentration. The Langmuir Eq. (19) is, as shown in Fig. 8, better fitted with data at high concentration range but poorly fitted at low concentration range. Usually, the ratio of influent to effluent concentration of the adsorption process is about 100. Langmuir equation generally cannot accommodate itself to a wide concentration range. Though concentrations decrease from high to low in the adsorption process, the adsorption equilibrium is at low concentration range. The inevitable deviation at low concentration range from Langmuir equation causes errors in engineering evaluation. Priority consideration should be given to the Freundlich equation for adsorption equilibrium design at low concentration range.

The Langmuir equation is more accurate at high concentration range. It is frequently used for evaluating the quality of the adsor-

bent. Especially its q_{mon} value is frequently used as an indicator for evaluating an adsorption system. The q_{mon} values of the adsorptions of three dyes on activated carbon studied increased linearly with increased KOH/char value as shown in Fig. 8. Fig. 8 also shows that the slope of adsorption of dye is steeper than the adsorption of phenol. The q_{mon} values of the adsorption of three dyes (MB, BB1, AB74) and three phenols (phenol, 4-CP, 2,4-DCP) on PKKC 40 are, respectively, 941, 1405, 388, 309, 582, and 759 g/kg, the highest values of this study and higher than values in literature (not shown).

Activated carbon in the studied series had another characteristic, i.e. the adsorption quantity per unit area of activated carbon in this studied series was almost the same as for any other adsorbate as shown in Fig. 9, which shows the plot of q_{mon}/S_p against KOH/char. The line of adsorption quantity of any adsorbate appears almost horizontal, implying almost equal adsorption capability per unit area of all activated carbons in the series. This is also characteristic of chemically KOH-activated carbon [21]. Usually, when activated carbon is prepared with the same method but at different activation levels (temperature, time, dose), the physical properties of pores (pore size distribution, pore characteristic) and chemical properties (chemical constituent, surface functional group) will all be affected, which, in turn, affects the adsorption amount of unit surface area of activated carbon. In the case of the activated carbon prepared from plant material with chemical KOH-activation, its chemical constituents and surface functional groups increase with increased surface area [21]; pore size decreases with increased surface area. BET surface areas of the activated carbons studied increase from 784 to 1725 m^2/g, while pore sizes decrease from 2.5 to 2.2 nm. There are still other factors (such as structure of carbon material or crystallization level) that are not investigated yet. All these factors affect the adsorption capability and make the adsorption capability of unit surface area of the activated carbons in the series are almost similar.

3.6. Design and operation of a countercurrent two- or three-stage adsorption system

In this section, adsorption of six adsobates on the activated carbon PKKC30 in the study are used as examples to calculate adsorbent consumption and middle concentrations of single-stage as well as countercurrent two- and three-stage systems for adsorption process selection. Procedures and explanations follow:

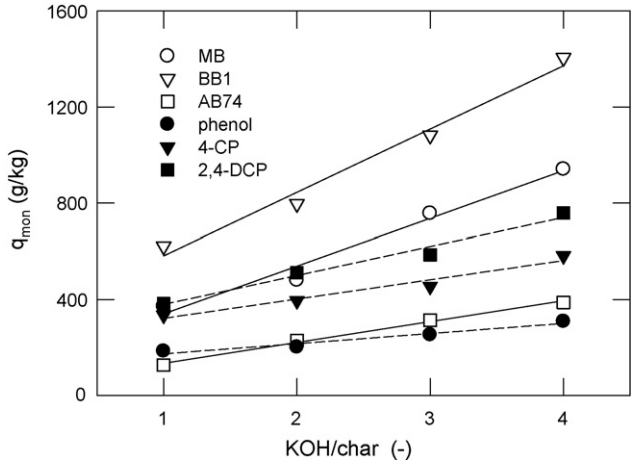

Fig. 8. Plot of q_{mon} against KOH/char ratio of activated carbon (adsorbates are MB (○), BB1 (▽), AB74 (□), phenol (●), 4-CP (▼) and 2,4-DCP (■), respectively).

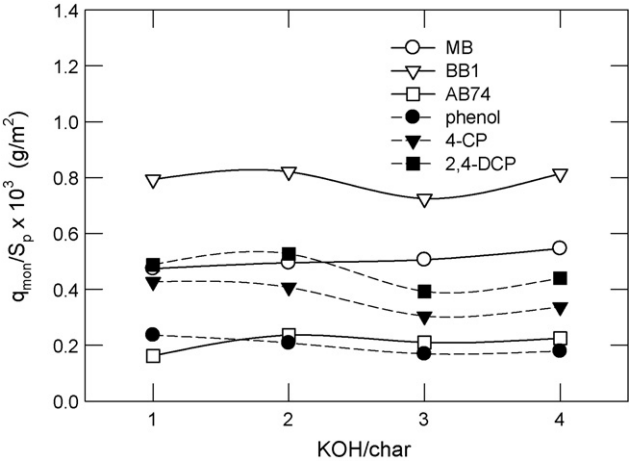

Fig. 9. Plot of q_{mon}/S_p against KOH/char ratio of activated carbon (adsorbates are MB (○), BB1 (▽), AB74 (□), phenol (●), 4-CP (▼) and 2,4-DCP (■), respectively).

1. Data obtained from isotherm equilibrium analysis of the adsorption system are listed (K_F and $1/n$ values of Freundlich equation) in Table 7.

   The influent and effluent concentrations (C_i and C_f) were inputted under operation conditions according to the operation requirements. In this study the effluent concentration (C_f) was designed as $1/100C_i$.
2. Eq. (3) is rewritten as

$$m_{x_s} = \frac{C_i - C_f}{K_F C_f^{1/n}} \tag{21}$$

   and adsorbent consumption (m_{x_s}) of a single-stage system is obtained from Eq. (21).
4. y_i, y_2, and y_f in Eqs. (9) and (10) are replaced with C_i, C_2, and C_f, respectively. Middle concentration C_2 is obtained from solving Eq. (9) by trial and error. Values of C_i, C_2, C_f and m_{x_s} are inserted in Eq. (10) and adsorbent consumption (m_{x_d}) for the countercurrent two-stage adsorption system is obtained.
5. y_i, y_2, y_3, y_f in Eqs. (15)–(17) are replaced with C_i, C_2, C_3, and C_f, respectively. Middle concentration C_2 and C_3 are obtained from solving simultaneously Eqs. (15) and (16) with trial and error. Values of C_i, C_2, C_3, C_f and m_{x_s} are then inserted in Eq. (17) to obtain adsorbent consumption (m_{x_t}) for the countercurrent three-stage adsorption system.
6. The above calculated values are show in Table 7. Compare values of m_{x_s}, m_{x_d}, and m_{x_t} and infer the suitable stage number. For example, in the adsorption system of BB1 on PKKC30, the adsorbent consumption of the single-stage system is 2.19 kg/m^3 and that of the countercurrent two-stage system is 0.877 kg/m^3, 1/2.5 that of the single-stage system, i.e. a saving of 60% adsorbent is obtained when a single-stage system is converted into a countercurrent two-stage system. The adsorbent consumption of the countercurrent three-stage system is 0.739 kg/m^3, 1/1.19 that of the two-stage one, i.e. a saving of 15% adsorbent is obtained when the three-stage system is used instead of the two-stage one.
7. The selected adsorption system can be designed and operated according to the procedures described in Section 3.2.

4. Conclusions

1. In this study, equilibrium-stage operations of liquid–solid phase single-stage, countercurrent two- and three-stage adsorption processes were deduced with the Freundlich equation. Calculations confirmed that less adsorbent was consumed for

countercurrent two- and three-stage adsorption systems than for a single-stage system.

2. Based on the assumption that a 25% adsorbent saving is equivalent to one increased stage, a suitable operation number of stages is obtained as: when $1/n \leq 0.05$, the single-stage system is suitable; when $0.05 < 1/n \leq 0.3$, the countercurrent two-stage system; when $0.3 < 1/n$, the countercurrent three-stage system.
3. About 56% of the $1/n$ values of literature collected were between 0.05 and 0.3 and about 44% of them were larger than 0.3, probably meaning that a countercurrent two- or three-stage adsorption system is needed for most of the adsorption systems. Furthermore, a set of countercurrent adsorption system was designed for practical operation. Detailed operation procedures together with the important notes are given.
4. Microporous activated carbons with specific areas of 290–1901 m^2/g were prepared from carbonized plum kernels activated at KOH/char ratios of 0–5. The Freundlich equation was better fitted to experimental data with smaller standard deviations. The 23 adsorption systems had $1/n$ values between 0.05 and 0.3 and 1 system had a $1/n$ value of less than 0.05. It was also clear that at low concentration range the Freundlich equation was better fitted to experimental data than Langmuir equation.
5. The q_{mon} values of the adsorptions of 3 dyes (MB, BB1, AB74) and 3 phenols (phenol, 4-CP, 2,4-DCP) on the activated carbon of KOH/char = 4 were, respectively, 941, 1405, 388, 309, 582, and 759 g/kg, proof of good adsorption capability.
6. Lastly a practical example was demonstrated to calculate the adsorption consumptions and middle solute concentrations of the single-stage, countercurrent two- and three-stage adsorption systems for determining the suitable number of stages and this provided as a reference for engineering design.

Acknowledgment

Financial support of this work by the National Science Council of the Republic of China under contract no. NSC 96-2221-E-239-021 is gratefully acknowledged.

References

[1] S. Veeraraghavan, L.T. Fan, Modeling adsorption in liquid–solid fluidized beds, Chem. Eng. Sci. 44 (1989) 2333–2344.
[2] C.B. Ching, K.H. Chu, K. Hidajat, Experimental study of a simulated countercurrent adsorption system. VII: Effects of non-linear and interacting isotherms, Chem. Eng. Sci. 48 (1993) 1343–1351.
[3] K. Kubota, C. Hata, S. Hayashi, A study of a simulated moving bed adsorber based on the axial dispersion model, Can. J. Chem. Eng. 67 (1989) 1025–1029.
[4] K.H. Chu, M.A. Hashim, Simulated countercurrent adsorption processes: a comparison of modeling strategies, Chem. Eng. J. 56 (1995) 59–65.
[5] S. Huang, R.W. Carr, A simple adsorber dynamics approach to simulated countercurrent moving bed reactor performance, Chem. Eng. J. 82 (2001) 87–94.
[6] H. Schmidt-Traub, J. Strube, Dynamic simulation of simulated-moving-bed chromatographic processes, Comput. Chem. Eng. 20 (1996) 641–646.
[7] C. Migliorini, M. Mazzotti, M. Morbidelli, Continuous chromatographic separation through simulated moving beds under linear and nonlinear conditions, J. Chromatogr. A 827 (1998) 161–173.
[8] J. Strube, H. Schmidt-Traub, Dynamic simulation of simulated-moving-bed chromatographic processes, Comput. Chem. Eng. 22 (1998) 1309–1317.
[9] K. Hashimoto, S. Adachi, H. Noujima, H. Maruyama, Models for the separation of glucose/fructose mixture using a simulated moving-bed, J. Chem. Eng. Jpn. 16 (1983) 400–406.
[10] K. Hashimoto, M. Yamada, Y. Shirai, Continuous separation of glucose-salts mixture with nonlinear and linear adsorption isotherms by using a simulated moving-bed adsorber, J. Chem. Eng. Jpn. 20 (1987) 405–410.
[11] K. Hashimoto, M. Yamada, S. Adachi, Y. Shirai, A Simulated moving-bed adsorber with three zones for continuous separation of L-phenylanine and NaCl, J. Chem. Eng. Jpn. 22 (1989) 432–434.
[12] K. Hashimoto, Y. Shirai, M. Morishita, S. Adachi, Continuous separation of glycerol and NaCl with linear and unfavorable adsorption isotherms by use of a simulated moving-bed adsorber, J. Chem. Eng. Jpn. 25 (1992) 453–455.
[13] K. Hashimoto, Y. Shirai, S. Adachi, A simulated moving-bed adsorber for the separation of tricomponents, J. Chem. Eng. Jpn. 26 (1993) 52–56.
[14] S. Kishihara, H. Horikawa, H. Tamaki, S. Fujii, Continuous chromatographic separation of palatinose (6-*o*-α-D-glucopyranosyl-D-fructose) and trehalulose (1-*o*-α-D-glucopyranosyl-D-fructose) using a simulated moving-bed adsorber, J. Chem. Eng. Jpn. 22 (1989) 434–436.
[15] K.B. Kim, S. Kishihara, S. Fujii, Simultaneously continuous separation of glucose, maltose, and maltotriose using a simulated moving-bed adsorber, Biosci. Biotech. Biochem. 56 (1992) 801–802.
[16] M.M. Hassan, K.F. Loughlin, M.E. Biswas, Optimization of continuous countercurrent adsorption systems, Sep. Purif. Technol. 6 (1996) 19–27.
[17] R.L. Tseng, F.C. Wu, R.S. Juang, Liquid-phase adsorption of dyes and phenols using pinewood-based activated carbons, Carbon 41 (2003) 487–495.
[18] M.A. Lillo-Rodenas, D. Logano-Castello, D. Cazorla-Amoros, A. Linares-Solano, Preparation of activated carbons from Spanish anthracite. II: Activation by NaOH, Carbon 39 (2001) 751–759.
[19] A.A. El-Hendawy, S.E. Samra, B.S. Girgis, Adsorption characteristics of activated carbons obtained from corncobs, Colloid Surf. A180 (2001) 209–221.
[20] M. Suzuki, Elsevier, in: Adsorption Engineering, Kodansha Ltd., Tokyo, 1990.
[21] R.L. Tseng, S.K. Tseng, Characterization and use of high surface area activated carbons prepared from cane pith for liquid-phase adsorption, J. Hazard. Mater. B136 (2006) 671–680.
[22] E.N.E. Qada, S.J. Allen, G.M. Walker, Adsorption of methylene blue onto activated carbon produced from steam activated bituminous coal: a study of equilibrium adsorption isotherm, Chem. Eng. J. 124 (2006) 103–110.
[23] P.C.C. Faria, J.J.M. Orfao, M.F.R. Pereira, Adsorption of anionic and cationic dyes on activated carbons with different surface chemistries, Water Res. 38 (2004) 2043–2053.
[24] A. Jumasiah, T.G. Chuah, J. Gimbon, T.S.Y. Choong, I. Azni, Adsorption of basic dye onto palm kernel shell activated carbon: sorption equilibrium and kinetics studies, Desalination 186 (2005) 57–64.
[25] O. Gercel, A. Ozcan, A. Safa Ozcan, H. Ferdi Gercel, Preparation of activated carbon from a renewable bio-plant of *Euphorbia rigida* by H_2SO_4 activation and its adsorption behavior in aqueous solutions, Appl. Surf. Sci. 253 (2007) 4843–4852.
[26] B.G.P. Kumar, L.R. Miranda, M. Velan, Adsorption of Bismark Brown dye on activated carbons prepared from rubberwood sawdust using different activation methods, J. Hazard. Mater. B 126 (2005) 63–70.
[27] P.C.C. Faria, J.J.M. Órfão, M.F.R. Pereira, Adsorption of anionic and cationic dyes on activated carbons with different surface chemistries, Water Res. 38 (2004) 2043–2052.
[28] G. McKay, Adsorption of dyestuffs from aqueous solutions with activated carbon. I: Equilibrium and batch contact-time studies, J. Chem. Technol. Biot. 32 (1982) 759–772.
[29] Z. Hu, M.P. Srinivasan, Y. Ni, Novel activation process for preparing highly microporous and mesoporous activated carbon, Carbon 39 (2001) 877–886.
[30] V. Meshko, L. Markovska, M. Mincheva, A.E. Rodrigues, Adsorption of basic dyes on granular activated carbon and natural zeolite, Water Res. 35 (2001) 3357–3366.
[31] W.T. Tsai, C.Y. Chang, M.C. Lin, S.F. Chien, H.F. Sun, M.F. Hsieh, Adsorption of acid dye onto activated carbons prepared from agricultural waste bagasse by $ZnCl_2$ activation, Chemosphere 45 (2001) 51–58.
[32] R. Malik, D.S. Ramteke, S.R. Wate, Adsorption of malachite green on groundnut shell waste based powdered activated carbon, Waste Manage. 27 (2007) 1129–1138.
[33] A-N.A. El-Hendawy, S.E. Samra, B.S. Girgis, Adsorption characteristics of activated carbons obtained from corncobs, Colloid Surf. A 180 (2001) 209–221.
[34] M. Valix, W.H. Cheung, G. McKay, Preparation of activated carbon using low temperature carbonization and physical activation of high ash raw bagasse for acid dye adsorption, Chemosphere 56 (2004) 493–501.
[35] X. Yang, B. Al-Duri, Kinetic modeling of liquid-phase adsorption of reactive dyes on activated carbon, J. Colloid Interf. Sci. 287 (2005) 25–34.
[36] A-N.A. El-Hendawy, Influence of HNO_3 oxidation on the structure and adsorptive properties of corncob-based activated carbon, Carbon 41 (2003) 713–722.
[37] A.M. Warhurst, G.L. McConnachie, S.J.T. Pollard, Characterisation and applications of activated carbon produced from *Moringa oleifera* seed husks by single-step steam pyrolysis, Water Res. 31 (1997) 759–766.
[38] N. Hoda, E. Bayram, E. Ayranci, Kinetic and equilibrium studies on the removal of acid dyes from aqueous solutions by adsorption onto activated carbon cloth, J. Hazard. Mater. B137 (2006) 344–351.
[39] P.K. Malik, Dye removal from wastewater using activated carbon developed from sawdust: adsorption equilibrium and kinetics, J. Hazard. Mater. B 113 (2004) 81–88.
[40] P.K. Malik, Use of activated carbons prepared from sawdust and rice-husk for adsorption of acid dyes: a case study Acid Yellow 36, Dyes Pigments 56 (2003) 239–249.
[41] A. Namane, A. Mekarzia, K. Benrachedi, N. Belhaneche-Bensemra, A. Hellal, Determination of the adsorption capacity of activated carbon made from coffee ground by chemical activation with $ZnCl_2$ and H_3PO_4, J. Hazard. Mater. B119 (2005) 189–194.
[42] K.V. Kumar, S. Sivanesan, Isotherm parameters for basic dyes onto activated carbon: comparison of linear and non-linear method, J. Hazard. Mater. B 129 (2006) 147–150.

[43] A. Aygun, S. Yenisoy-Karakas, I. Duman, Production of granular activated carbon from fruit stones and nutshells and evaluation of their physical, chemical and adsorption properties, Microporous Mesoporous Mater. 66 (2003) 189–195.
[44] A.-N.A. El-Hendawy, Surface and adsorptive properties of carbons prepared from biomass, Appl. Surf. Sci. 252 (2005) 287–295.
[45] I.D. Mall, V.C. Srivastava, N.K. Agarwal, I.M. Mishra, Adsorptive removal of malachite green dye from aqueous solution by bagasse fly ash and activated carbon-kinetic study and equilibrium isotherm analyses, Colloid Surf. A 264 (2005) 17–28.
[46] T.G. Chuah, A. Jumasiah, I. Azni, S. Katayon, S.Y.T. Choong, Rice husk as a potentially low-cost biosorbent for heavy metal and dye removal: an overview, Desalination 175 (2005) 305–316.
[47] Y. Bulut, N. Gozubenli, H. Aydin, Equilibrium and kinetics studies for adsorption of direct blue 71 from aqueous solution by wheat shells, J. Hazard. Mater. 144 (2007) 300–306.
[48] M.T. Sulak, E. Demirbas, M. Kobya, Removal of Astrazon Yellow 7GL from aqueous solutions by adsorption onto wheat bran, Bioresour. Technol. 98 (2007) 2590–2598.
[49] Z. Eren, F.N. Acar, Adsorption of reactive black 5 an aqueous solution: equilibrium and kinetic studies, Desalination 194 (2006) 1–10.
[50] N.A. Zeid, G. Nakhla, S. Farooq, E. Osei-Twum, Activated carbon adsorption in oxidizing environments, Water Res. 29 (1995) 653–660.
[51] H. Moon, W.K. Lee, Intraparticle diffusion in liquid-phase adsorption of phenols with activated carbon in finite batch adsorber, J. Colloid Interf. Sci. 96 (1983) 162–172.
[52] F.C. Wu, R.L. Tseng, R.S. Juang, Comparisons of porous and adsorption properties of carbons activated by steam and KOH, J. Colloid Interf. Sci. 283 (2005) 49–56.
[53] O. Aktas, F. Cecen, Adsorption, desorption and bioregeneration in the treatment of 2-chlorophenol with activated carbon, J. Hazard. Mater. 141 (2007) 769–777.
[54] M. Streat, J.W. Patrick, M.J.C. Perez, Sorption of phenol and para-chlorophenol and novel activated carbons, Water Res. 29 (1995) 467–472.
[55] K. Laszlo, Adsorption from aqueous phenol and aniline solutions on activated carbons with different surface chemistry, Colloid Surf. A 265 (2005) 32–39.
[56] Q. Qian, M. Machida, H. Tatsumoto, Preparation of activated carbons from cattle-manure compost by zinc chloride activation, Bioresour. Technol. 98 (2007) 353–360.
[57] A. Dabrowski, P. Podkoscielny, Z. Hubicki, M. Barczak, Adsorption of phenolic compounds by activated carbon—a critical review, Chemosphere 58 (2005) 1049–1070.
[58] S.J.T. Pollard, F.E. Thompson, G.L. McConnachie, Microporous carbons from *Moringa oleifera* husks for water purification in less developed countries, Water Res. 29 (1995) 337–347.
[59] M.W. Jung, K.H. Ahn, Y. Lee, K.P. Kim, J.S. Rhee, J.T. Park, K.J. Paeng, Adsorption characteristics of phenol and chlorophenols on granular activated carbons (GAC), Microchem. J. 70 (2001) 123–131.
[60] N. Roostaei, H. Tezel, Removal of phenol from aqueous solutions by adsorption, J. Environ. Manage. 70 (2004) 157–164.
[61] M. Radhika, K. Palanivelu, Adsorptive removal of chlorophenols from aqueous solution by cost adsorbent-kinetics and isotherm analysis, J. Hazard. Mater. B138 (2006) 116–124.
[62] X. Chen, S. Jeyaseelan, N. Graham, Physical and chemical properties study of the activated carbon made from sewage sludge, Waste Manage. 22 (2002) 755–760.
[63] J.P. Wang, H.M. Feng, H.Q. Yu, Analysis of adsorption characteristics of 2,4-dichlorophenol from aqueous solution by activated carbon fiber, J. Hazard. Mater. 144 (2007) 200–207.
[64] B. Ozkaya, Adsorption and desorption of phenol on activated carbon and a comparison of isotherm models, J. Hazard. Mater. B129 (2006) 158–163.
[65] M. Tomaszewska, S. Mozia, A.W. Morawski, Removal of organic matter coagulation enhanced with adsorption on PAC, Desalination 161 (2004) 79–87.
[66] S. Rengaraj, S.H. Moon, R. Sivabalan, B. Arabindoo, V. Murugesan, Removal of phenol from aqueous solution and resin manufacturing industry wastewater using an agricultural waste: rubber seed coat, J. Hazard. Mater. B89 (2002) 185–196.
[67] I.I. Salame, T.J. Bandosz, Role of surface chemistry in adsorption of phenol on activated carbons, J. Colloid Interf. Sci. 264 (2003) 307–312.
[68] N.R. Khalili, J.D. Vyas, W. Weangkaew, S.J. Westfall, S.J. Parulekar, R. Sherwood, Synthesis and characterization of activated carbon and bioactive adsorbent produced from paper mill sludge, Sep. Purif. Technol. 26 (2002) 295–304.